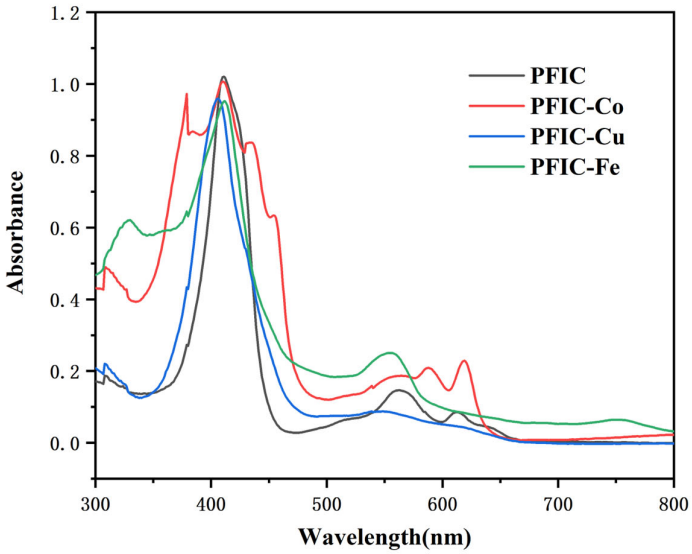

Figure S1. UV-vis spectrum of PFIC and PFIC-Co, PFIC-Cu and PFIC-Fe in CH_2Cl_2.

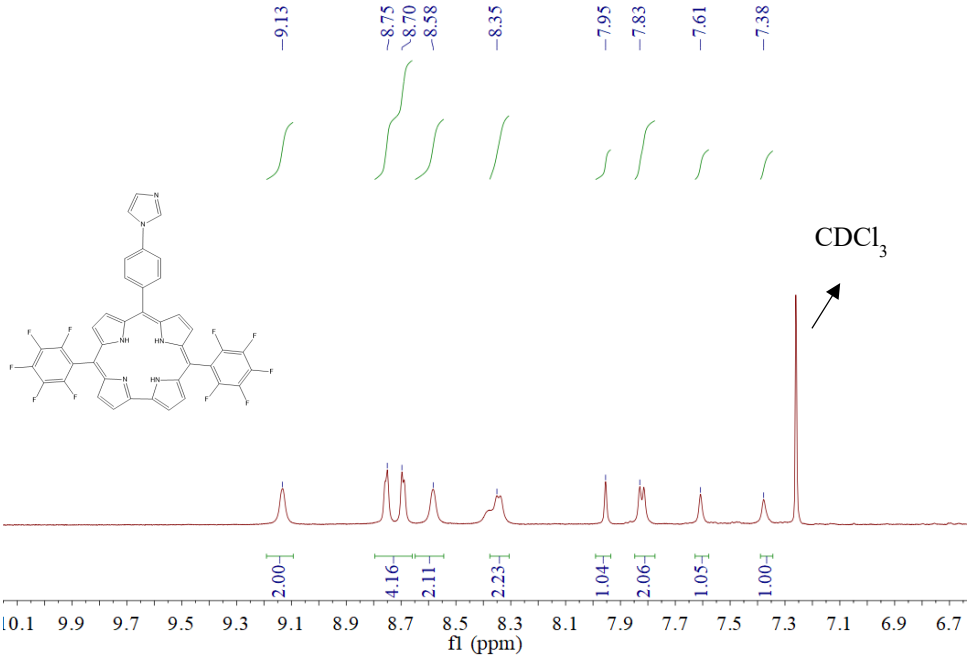

Figure S2. ^1H NMR spectrum of 5,15-bis-(pentafluorophenyl)-10- [4-(1H-imidazole) phenyl]-corrole.

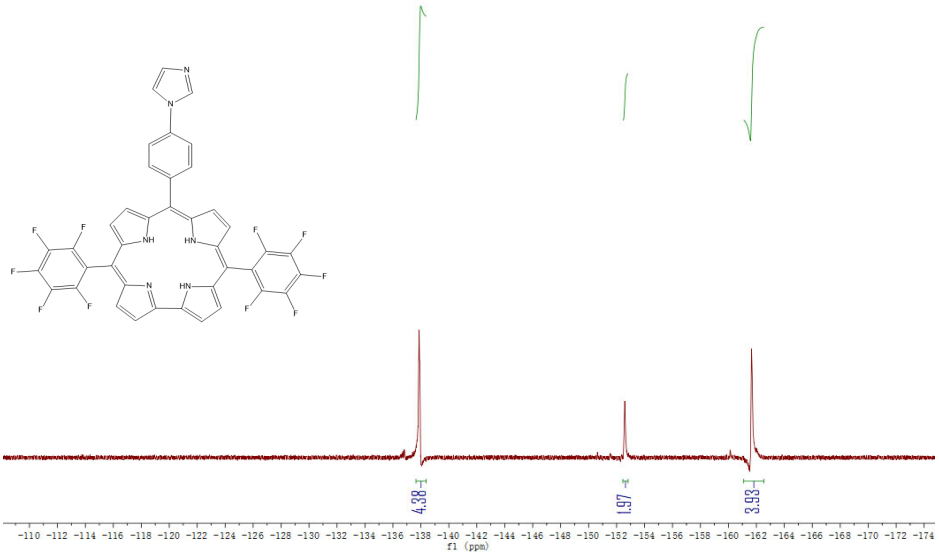

Figure S3. ^{19}F NMR spectrum of 5,15-bis-(pentafluorophenyl)-10-[4-(1H-imidazole) phenyl]-corrole.

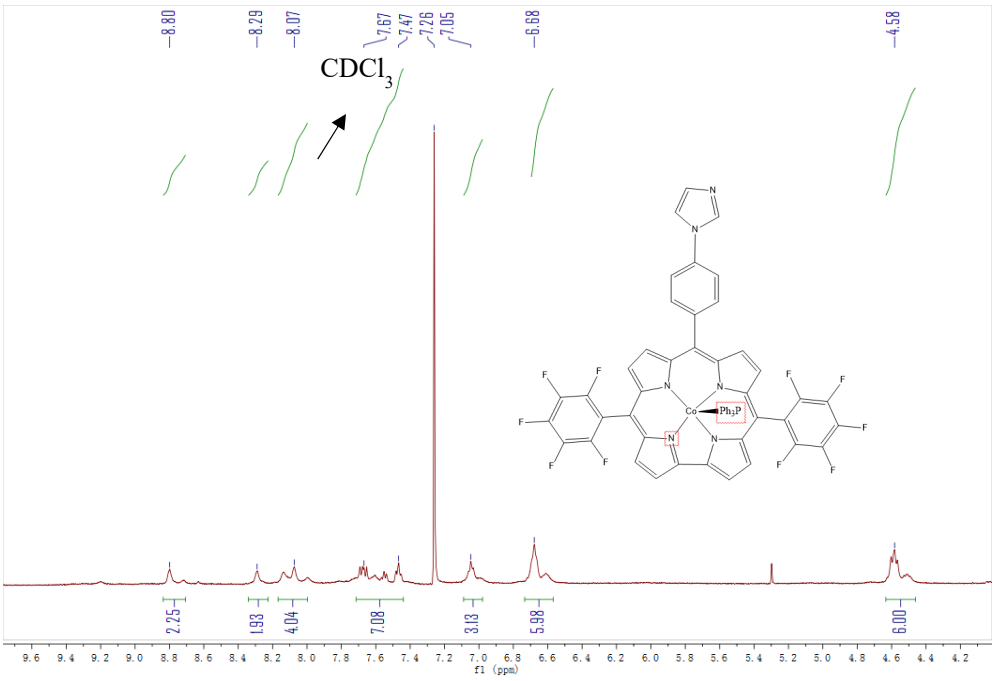

Figure S4. ^{1}H NMR spectrum of cobalt 5,15-bis-(pentafluorophenyl)-10-[4-(1H-imidazole) phenyl]-corrole.

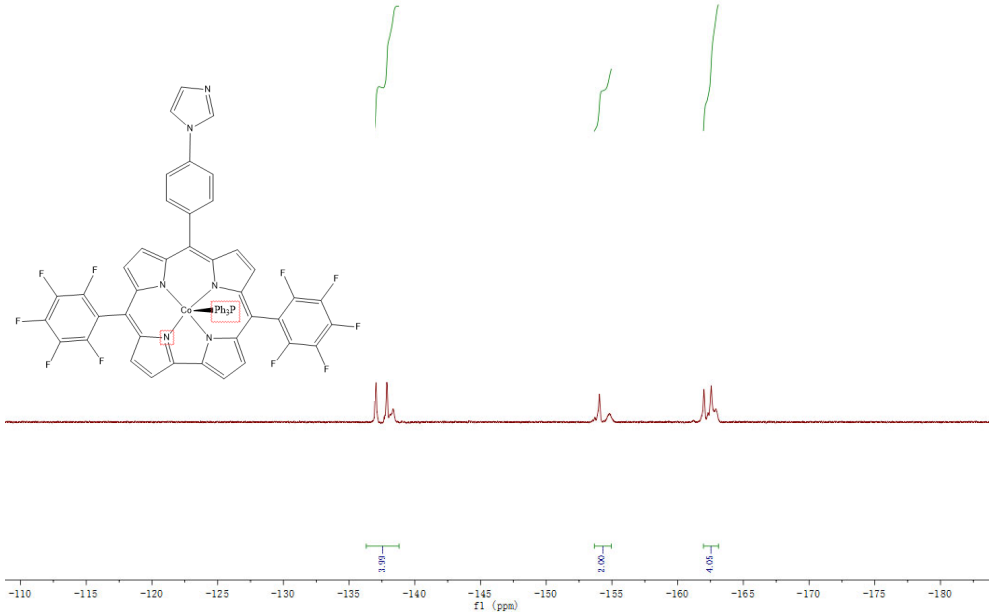

Figure S5. ^{19}F NMR spectrum of cobalt 5,15-bis-(pentafluorophenyl)-10-[4-(1H-imidazole) phenyl]-corrole.

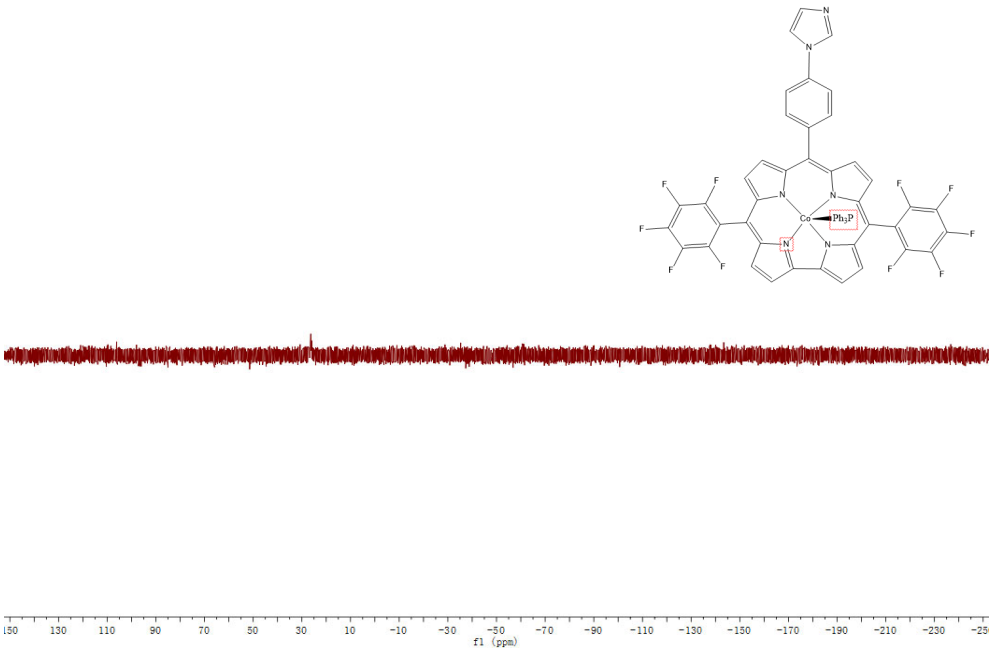

Figure S6. ^{31}P NMR spectrum of cobalt 5,15-bis-(pentafluorophenyl)-10-[4-(1H-imidazole) phenyl]-corrole.

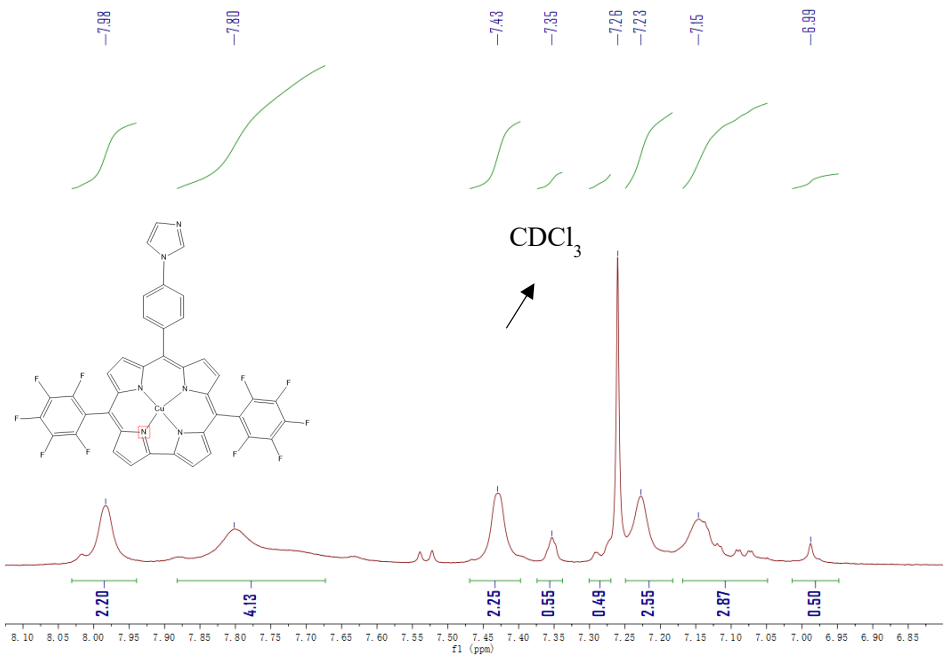

Figure S7. [1]H NMR spectrum of copper 5,15-bis-(pentafluorophenyl)-10-[4-(1H-imidazole) phenyl]-corrole. .

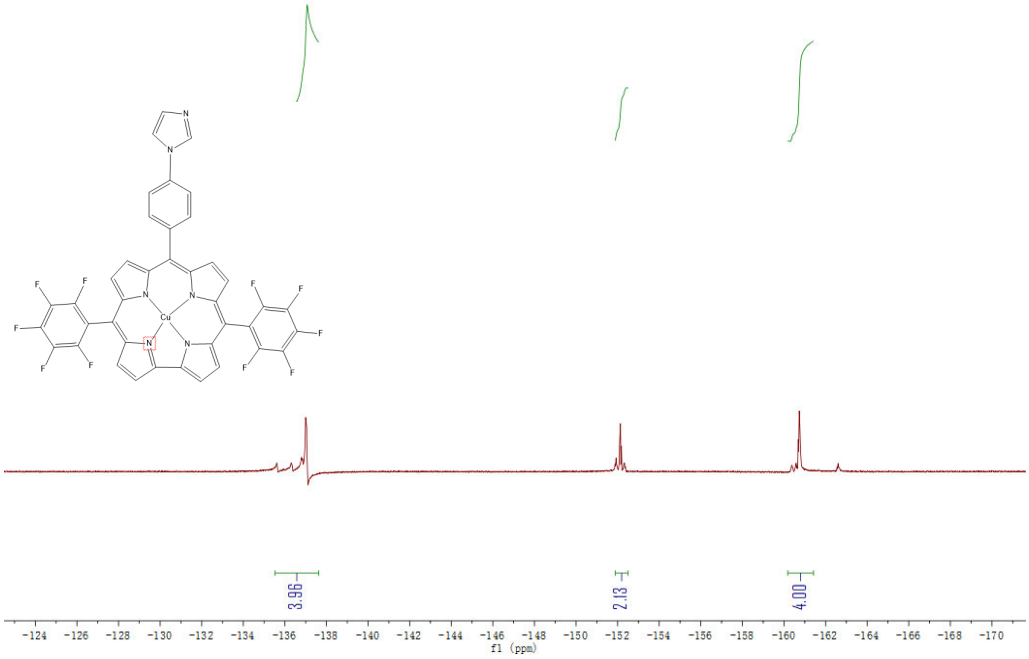

Figure S8. [19]F NMR spectrum of copper 5,15-bis-(pentafluorophenyl)-10-[4-(1H-imidazole) phenyl]-corrole.

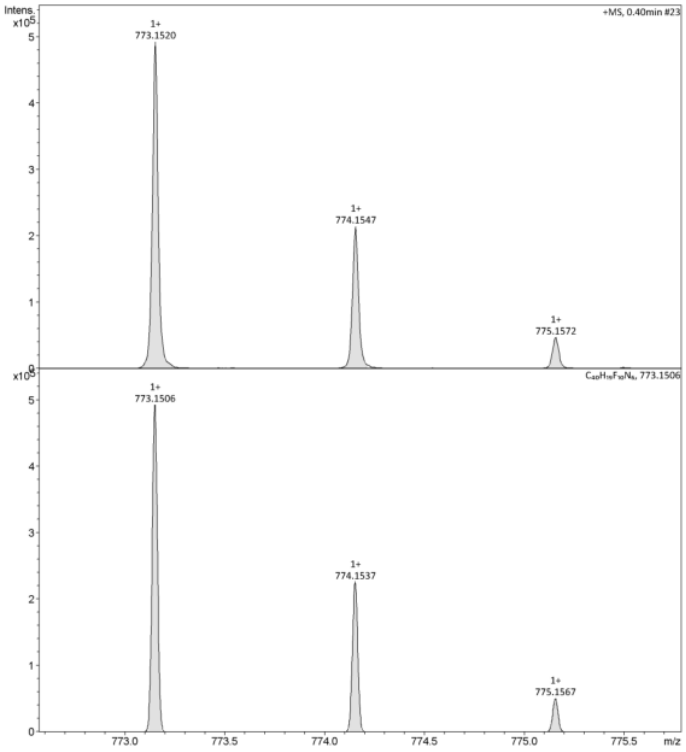

Figure S9. High resolution mass spectrum of 5,15-bis-(pentafluorophenyl)-10-[4-(1H-imidazole) phenyl]- corrole.

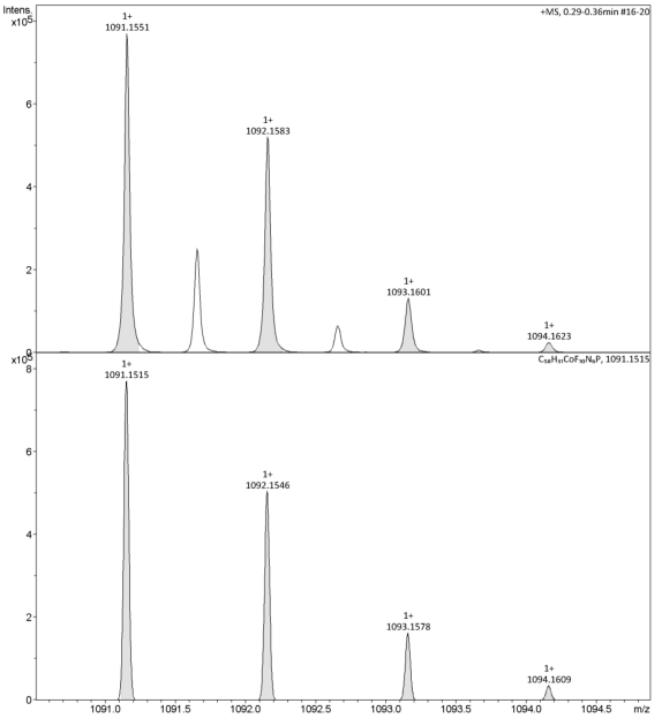

Figure S10. High resolution mass spectrum of cobalt 5,15-bis-(pentafluorophenyl)-10-[4-(1H-imidazole) phenyl]- corrole.

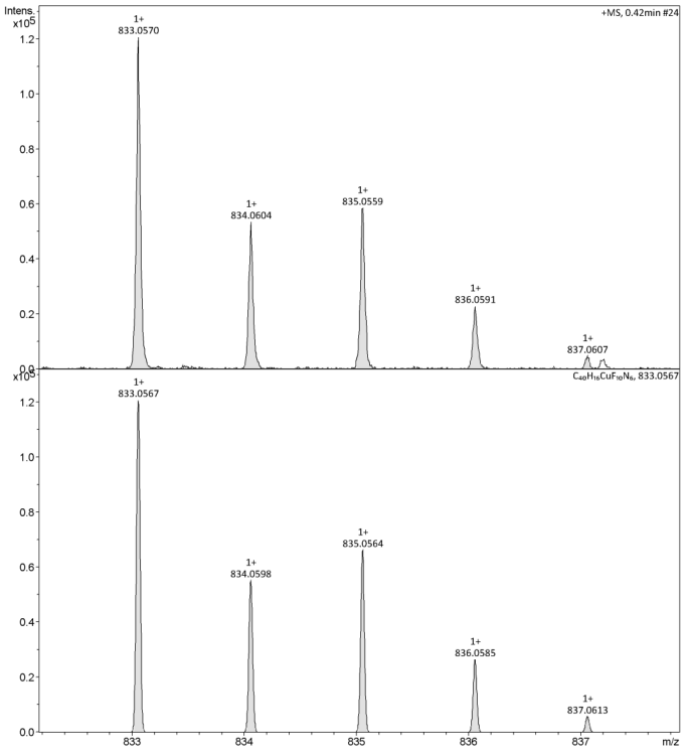

Figure S11. High resolution mass spectrum of copper 5,15-bis-(pentafluorophenyl)-10-[4-(1H-imidazole) phenyl]- corrole.

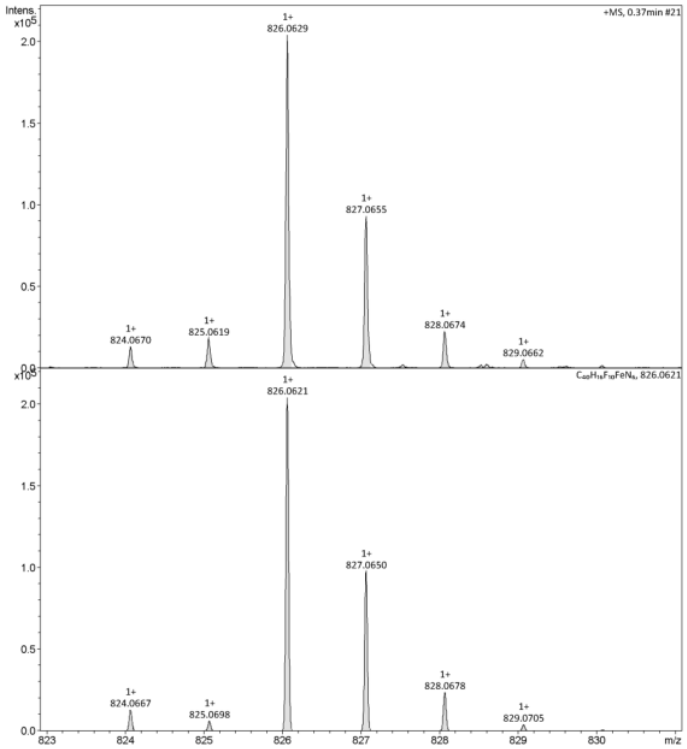

Figure S12. High resolution mass spectrum of iron 5,15-bis-(pentafluorophenyl)-10-[4-(1H-imidazole) phenyl]- corrole.

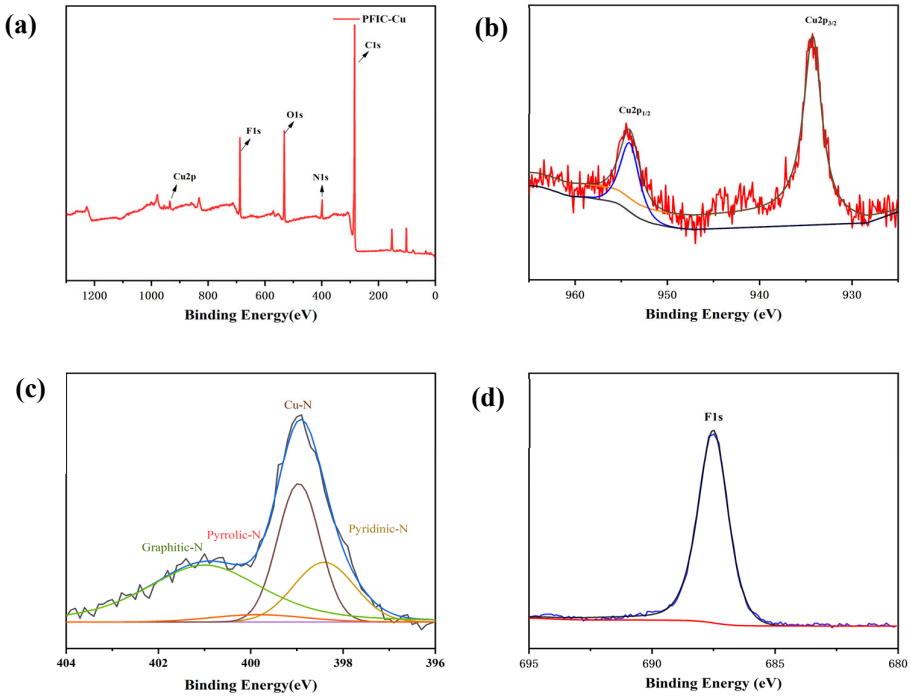

Figure S13. XPS survey spectrum of **PFIC-Cu** (a); XPS spectra of Cu 2p (b) and N 1s (c) and F 1s (d) of **PFIC-Cu.**

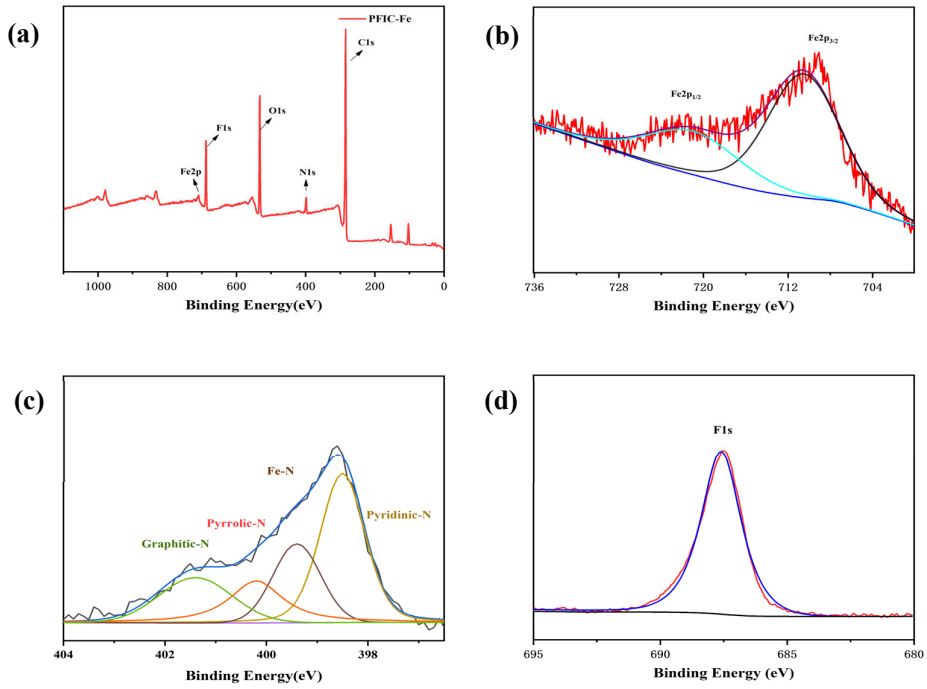

Figure S14. XPS survey spectrum of **PFIC-Fe** (a); XPS spectra of Fe 2p (b) and N 1s (c) and F 1s (d) of **PFIC-Fe.**

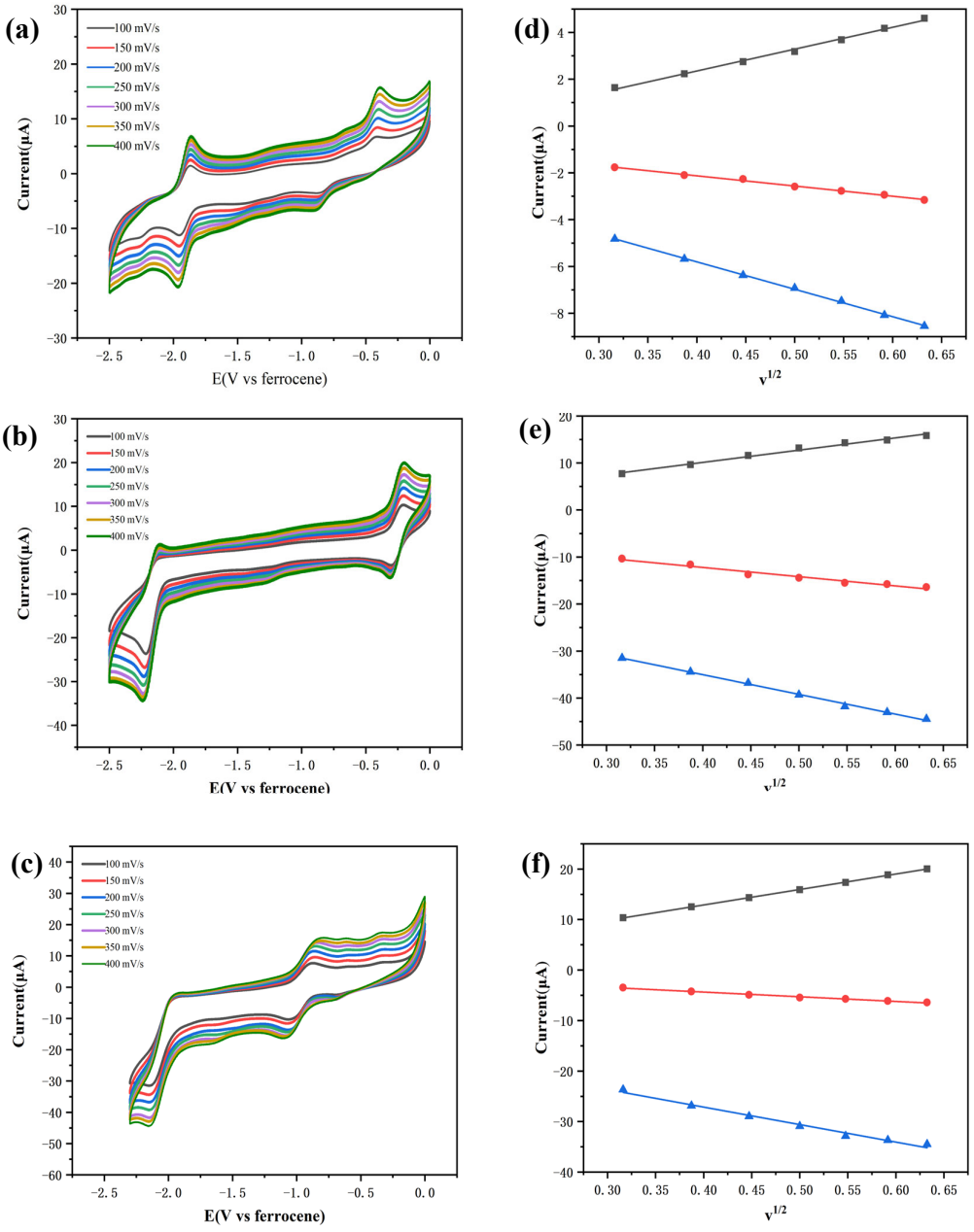

Figure S15. Plots of metal corrole complexes Co, Cu, and Fe (a-c, 1.0 mM) for sweep rate (v) variations of 100-400 mV/s and peak currents (i_P) versus square root of the sweep rate ($v_{1/2}$) for the reduction and first oxidation peaks (d-f).

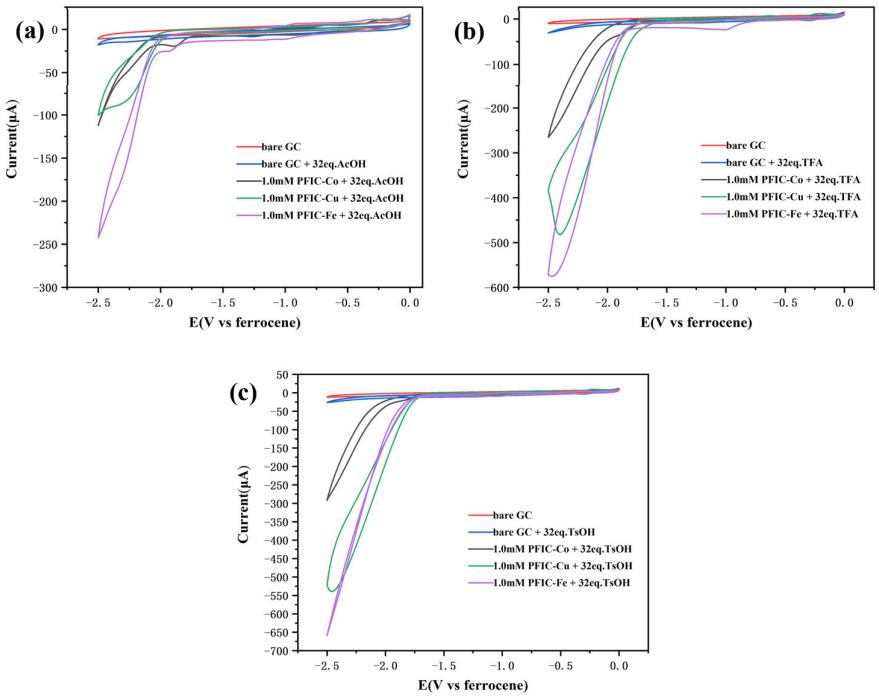

Figure S16. Comparison of CV test between bare GC and PFIC-Co, PFIC-Cu and PFIC-Fe at high acid concentration.

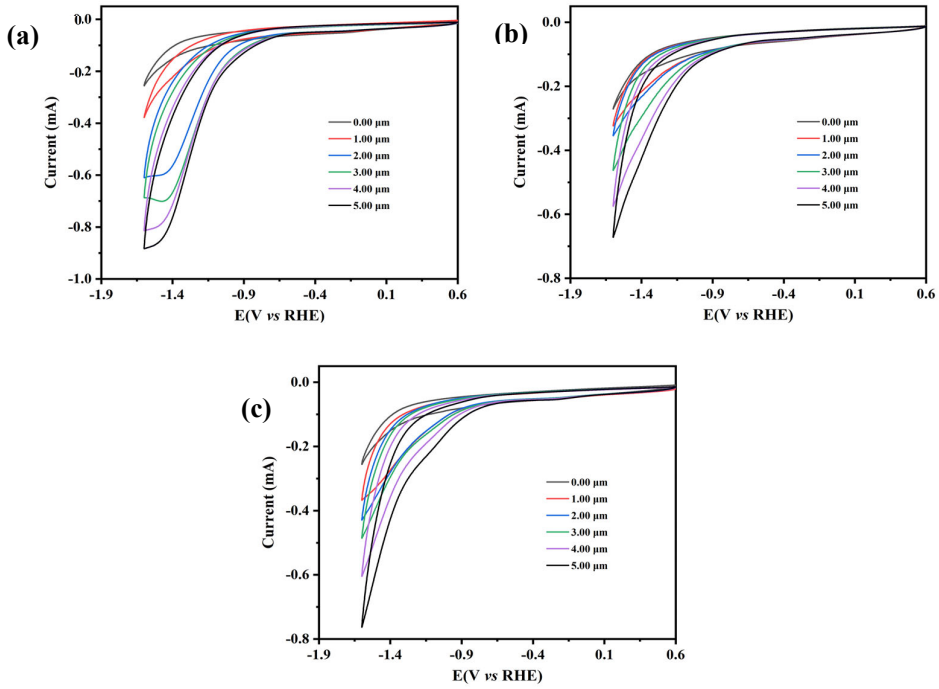

Figure S17. CV plots (0.00-5.00 μM) of different concentrations of metallcorrole complexes (PFIC-Co(a), PFIC-Cu(b), PFIC-Fe(c)) in a mixed system of acetonitrile and water (pH = 7).

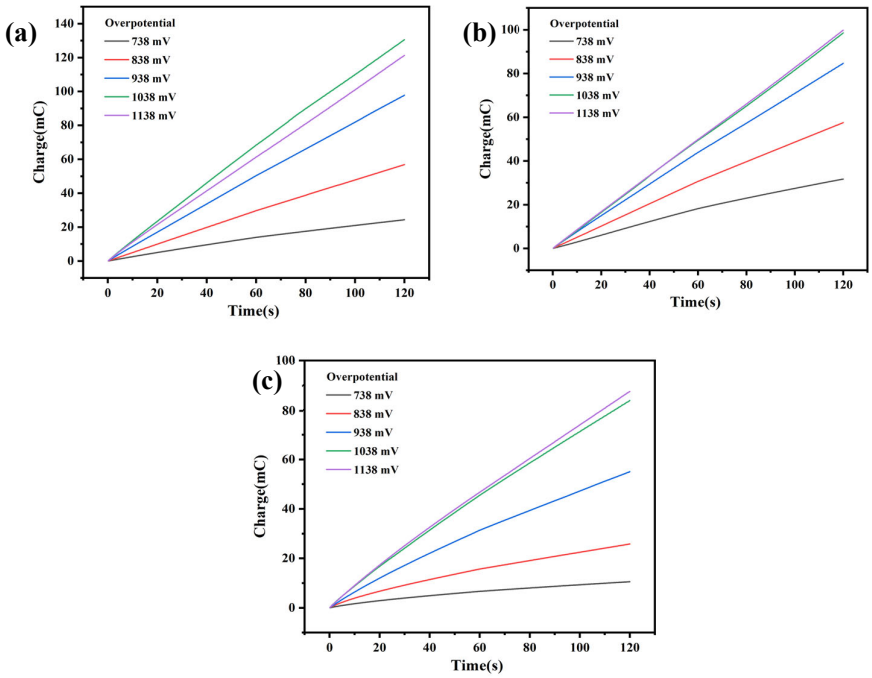

Figure S18. (a) Charge increase for **PFIC-Co** (5.00 μM), (b) Charge increase for **PFIC-Cu** (5.00 μM), (c) Charge increase for **PFIC-Fe** (5.00 μM) at different overpotentials.

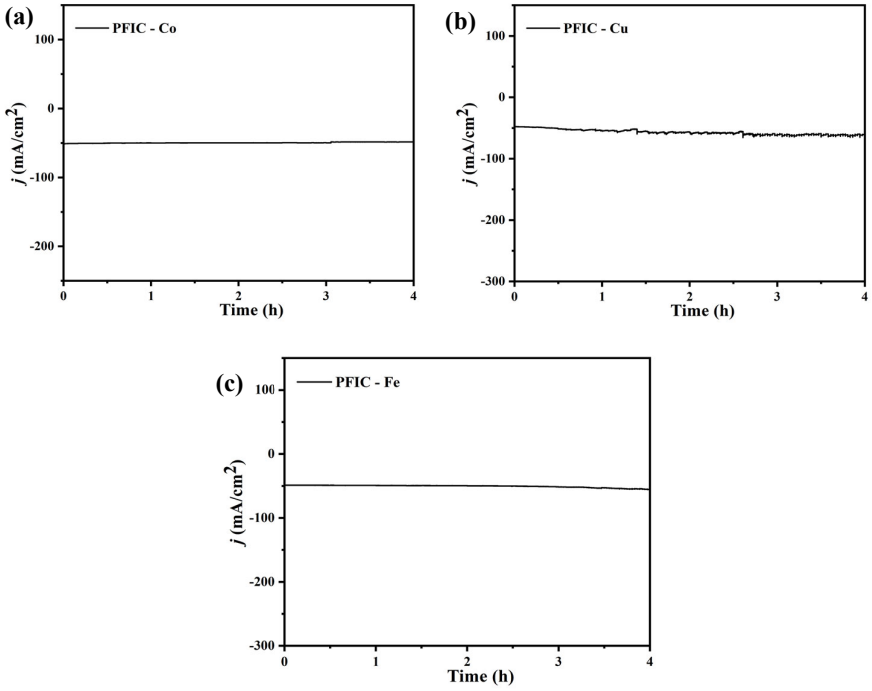

Figure S19. Catalytic current versus time obtained from 4 h CPE with 5.00 μM (a) PFIC -Co, (b) PFIC – Cu (c) PFIC-Fe in buffer solution at -1.04 V vs. RHE.

Table S1. Crystal data and structure refinement for **PFEC-Co.**

Identification code	Cu
Empirical formula	$C_{46}H_{29}CuF_{10}N_6$
Formula weight	919.29
Temperature/K	100
Crystal system	monoclinic
Space group	$P2_1/n$
a/Å	18.0785(8)
b/Å	5.4994(2)
c/Å	39.0484(15)
α/°	90
β/°	90.15(5)
γ/°	90
Volume/Å^3	3882.2(3)
Z	4
ϱ_{calc}g/cm^3	1.573
μ/mm^{-1}	1.612
F(000)	1864.0
Crystal size/mm^3	0.08 × 0.05 × 0.04
Radiation	CuKα (λ = 1.54178)
2Θ range for data collection/°	4.526 to 127.79
Index ranges	-21 ≤ h ≤ 20, -6 ≤ k ≤ 6, -44 ≤ l ≤ 45
Reflections collected	21887
Independent reflections	6257 [R_{int} = 0.1202, R_{sigma} = 0.1010]
Data/restraints/parameters	6257/0/570
Goodness-of-fit on F^2	1.003
Final R indexes [I>=2σ (I)]	R_1 = 0.0747, wR_2 = 0.1864
Final R indexes [all data]	R_1 = 0.1170, wR_2 = 0.2189
Largest diff. peak/hole / e Å^{-3}	0.59/-0.91

Table S2. Catalytic performance parameters of three metal complexes in TFA system.

Complex	i_{cat}/i_p	**TOF, s $^{-1}$**	**Efficiency (C.E)**
PFIC-Co	30.40	217	0.95
PFIC-Cu	23.79	109	0.74
PFIC-Fe	25.42	125	0.79

Table S3. Catalytic performance parameters of three metal complexes in TsOH system.

Complex	i_{cat}/i_p	**TOF, s $^{-1}$**	**Efficiency (C.E)**
PFIC-Co	33.58	265	1.04
PFIC-Cu	26.76	138	0.84
PFIC-Fe	23.79	109	0.74

Table S4. HER activity for transition metal corroles in organic solvent by using organic acids as proton.

Catalysts	Proton source	Solvent	Onset potential (V)	Overpotential (mV)	TOF (s^{-1})	Refs.
PFIC-Co	TsOH	DMF	-1.71	780(10 μ A)	265	This work
PFIC-Cu	TsOH	DMF	-1.63	700(10 μ A)	138	This work
PFIC-Fe	TsOH	DMF	-1.81	880(10 μ A)	109	This work
((CF3)4 -tpfc) Cu	TFA	Acetonitrile	-1.85	1030(50 μ A)	227	[1]
PFEC-Fe	TFA	DMF	1.71	735(20 μ A)	13	[2]
(4-BPFC) Co	TsOH	DMF	-1.83	900(20 μ A)	93	[3]
(3-BPSC) Co	TsOH	DMF	-1.77	840(20 μ A)	187	[3]
Co (PBHC)	TsOH	DMF	-1.48	507(10 μ A)	203	[4]
Co (TPC)	TsOH	DMF	-1.56	630(10 μ A)	381	[5]
$Co(dmg)_2Cl$(pyridine)	MES	[illegible]	-1.43	515(10 μ A)	930	[6]
$Co(dmg)_2Cl$ (4-ethylamine pyridine)	MES	[illegible]	-1.11	457(10 μ A)	1350	[7]

Table S5. Faraday efficiency of transition metal complexes in nature homogeneous aqueous solution.

Complex	Faraday efficiency (%)	Solution	Refs.
PFIC-Co	94.7	Buffer	This work
PFIC-Cu	91.3	Buffer	This work
PFIC-Fe	89.8	Buffer	This work
((CF3)4 -tpfc) Cu	74	Water	[1]
PFEC-Fe	85.3	Buffer	[2]
Co (PBHC)	91.1	Buffer	[4]
Co (TPC)	98	Buffer	[5]
Co (BPCC)	92	Buffer	[5]
Fe (TPFC)Cl	93	Water	[8]
[Ni-en-P_2] $(ClO_4)_2$	93	Buffer	[9]

1. Sudhakar, K., et al., *Copper Complexes of CF3-Substituted Corroles for Affecting Redox Potentials and Electrocatalysis.* ACS Applied Energy Materials, 2020. **3**(3): p. 2828-2836.
2. Yadav, P., et al., *Hydrogen evolution catalysis by terminal molybdenum-oxo complexes.* iScience, 2021. **24**(8): p. 102924.
3. Dolganov, A.V., et al., *Control of the substituent at the nitrogen atom in a 2,4,6-triphenylpyridinium perchlorates tunes the electrocatalytic hydrogen evolution mechanism and efficiency.* International Journal of Hydrogen Energy, 2020. **45**(1): p. 501-507.
4. Lv, Z.-Y., et al., *Electrocatalytic Hydrogen Evolution of the Cobalt Triaryl Corroles Bearing Hydroxyl Groups.* 2023. **26**(12): p. e202200755.
5. Liu, Z.Y., et al., *Electrocatalytic hydrogen production by CN-substituted cobalt triaryl corroles.* Catalysis Science & Technology, 2022. **12**(16): p. 5125-5135.

6. Dolui, D., et al., *Enzyme-Inspired Synthetic Proton Relays Generate Fast and Acid-Stable Cobalt-Based H2 Production Electrocatalysts.* ACS Catalysis, 2019. **9**(11): p. 10115-10125.
7. Dolui, D., A.Q. Mir, and A. Dutta, *Probing the peripheral role of amines in photo- and electrocatalytic H_2 production by molecular cobalt complexes.* Chemical Communications, 2020. **56**(94): p. 14841-14844.
8. Zhong, Y.-Q., et al., *A comparative study of electrocatalytic hydrogen evolution by iron complexes of corrole and porphyrin from acetic acid and water.* Transition Metal Chemistry, 2019. **44**(5): p. 399-406.
9. Wang, C.-L., et al., *A new catalyst based on a nickel(II) complex of diiminodiphosphine for hydrogen evolution and oxidation.* International Journal of Hydrogen Energy, 2021. **46**(64): p. 32480-32489.